

Self-induced transparency mode-locking, and area theorem

R. M. Arkhipov

ITMO University, Kronverkskiy prospekt 49, 197101, St. Petersburg, Russia

M.V. Arkhipov

*Faculty of Physics, St. Petersburg State University,
Ulyanovskaya 1, Petrodvoretz, St. Petersburg 198504, Russia*

I. Babushkin

*Institute of Quantum Optics, Leibniz University Hannover, Welfengarten 1 30167, Hannover, Germany and
Max Born Institute, Max Born Str. 2a, Berlin, Germany*

N.N. Rosanov

Vavilov Optical State Institute, St. Petersburg, Russia

Self-induced transparency mode-locking (or coherent mode-locking, CML) which is based on intracavity self-induced transparency soliton dynamics, allows potentially to achieve nearly single cycle intracavity pulse durations, much below the phase relaxation time T_2 in a laser, which, despite of great promise, has not yet been realized experimentally. We develop a diagram technique which allows to predict the main features of CML regimes in a generic two-section laser. We show that CML can arise directly at the first laser threshold if the phase relaxation time is large enough. Furthermore, CML regimes can be unconditionally stable. We also predict the existence of “super-CML regimes”, with a pulse coupled to several Rabi oscillations in the nonlinear medium.

Ultrashort optical pulses with durations of a few hundreds femtoseconds (or picoseconds) are used in different applications ranging from real-time monitoring of chemical reactions to high-bit-rate optical communications [1]. The main technique to obtain such pulses nowadays is a passive mode-locking. The pulse duration in such lasers is fundamentally limited by the inverse bandwidth of the gain medium $\gamma_2 = 1/T_2$.

This very basic limitation is not valid anymore when the electric field is so strong, that Rabi oscillations in both gain and absorber sections are existed. The general idea of coherent modelocking (CML) [2–9] is that a self-induced transparency (SIT) soliton (or 2π pulse) [10–14] propagates stably in the absorber, whereas the gain section is arranged in such a way that the very same pulse (with the same shape) propagates there as a π pulse. Because of this, it “feeds” the energy from the gain medium [11–14], which makes it shorter. At the end, a stable equilibrium is set up due to balance of losses and gain, which defines finally the pulse duration. If the linear losses are small enough, the pulse duration will decrease until stopped by other mechanisms such as intracavity dispersion [15].

Up to now there were no clear experimental observation of the CML regime, although some work was made to improve theoretical description and to observe some elements of CML experimentally. At the same time, in [4, 5] the CML was predicted theoretically to quantum cascade lasers; in Ref. [16] experimental evidence of mode-locking regime in a laser with a coherent absorber has been reported (the gain section remained in incoherent regime).

In the present work, we show that CML might be easier accessible than was thought before. We develop a technique based on the well known McCall and Hahn area

theorem which determines the evolution of the pulse area in the CML laser. Using this technique we show that in a wide range of parameters CML regime is a stable attractor of the dynamics. We demonstrate furthermore the regimes we call super-CML where pulse area in absorber may approach $2n\pi$ for $n = 0$ and $n > 1$ instead of the only known case of $n = 1$. In order to keep the theory simple we will use the parameters where the pulse duration is far above the single-cycle pulse duration but still in the femtosecond range.

An important quantity describing the pulse dynamics in the coherent regime is the pulse area, defined as [11] $\Phi(t, z) = \frac{d}{\hbar} \int_{-\infty}^t \mathcal{E}(t', z) dt'$, where d is the transition dipole moment of two-level particles, and $\mathcal{E}(t, z)$ is the pulse envelope. The area Φ of a stable SIT-induced soliton is 2π . The basic result of the SIT theory is the so-called pulse area theorem. This theorem governs the evolution of the pulse area Φ during its propagation in a two-level absorbing (or amplifying) medium with an inhomogeneously broadened line [11–13]:

$$\frac{d\Phi}{dz} = -\frac{\alpha_0}{2} \sin \Phi, \quad (1)$$

where $\alpha_0 = \frac{8\pi^2 N_0 d^2 \omega_0 T_2^*}{\hbar c}$ is the absorption coefficient per unit length, N_0 is the concentration of two-level particles, ω_0 is the medium transition frequency and $\gamma_2^* = 1/T_2^*$ is the width of inhomogeneously broadened line. We remark that Eq. (1) is valid in the limit of negligible homogeneous broadening $T_2 \rightarrow \infty$. The solution of Eq. (1) is $\tan(\Phi/2) = \tan(\Phi_0/2) e^{-\alpha_0 z/2}$, where Φ_0 is the initial pulse area. $\Phi = \pi$ is an unstable steady-state of Eq. (1) whereas $\Phi = 0, 2\pi$ are stable ones. Coherent pulse propagation in an amplifying medium can be also described by

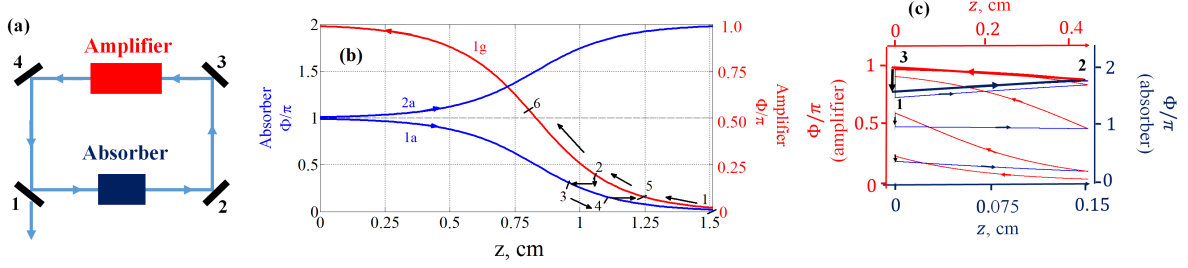


FIG. 1. (a): Schematic representation of mode-locked laser with a ring cavity where unidirectional counter clockwise lasing is assumed, 1, 2, 3, 4 are cavity mirrors, (b): Branches of solution of Eq.(1) for the absorber 1a, 2a (blue lines) and the amplifier 1g, 2g (red line) for $|\alpha_0| = 10 \text{ cm}^{-1}$, and (c): evolution of the pulse area Φ in the absorber and gain medium from the initial value $\Phi_0 = 0.025\pi$ to a limit cycle (thick arrows 123).

Eq. (1) simply assuming the opposite sign of α_0 . From Eq. (1) it follows that the same diagram can be used, only the opposite z -direction is to be taken. In this case, $\Phi = \pi$ is a stable point. Thus, a stable 2π soliton in an absorbing medium, and a stable π soliton in a gain medium can be formed.

Consider a CML laser operating in a unidirectional lasing regime shown in Fig. 1a with the absorbing and amplifying media separated in space. In order to achieve the same pulse shape for 2π -pulses and π -pulses in the absorber and amplifier respectively, one should take $d_a = 2d_g$, where $d_{a(g)}$ is the dipole moment of the absorber (amplifier) [2–9]. The branches of solutions of Eq. (1) in the amplifier and absorber are shown in Fig. 1b. Because of different dipole moments, these two branches are also different. Besides, as said, we reverse the sign of z to “mimic” the change of sign of α in Eq. (1). We choose the positive direction of motion in z as the pulse propagates in the absorber (blue curves noted as 1a, 2a), whereas for the amplifier the propagation direction is opposite (red curve noted as 1g).

Using such diagram technique we are able to understand easily the details of the pulse area evolution. In our laser in Fig. 1a a short pulse passes through the amplifier, is reflected from the mirror 1 with the reflection coefficient r , and then enters the absorber. We assume for simplicity that the other mirrors do not produce any energy loss. We also assume that the pulse travels long enough in every cavity section such that both the gain and absorber are able to recover to their equilibrium values between the pulse passages. Using the diagram in Fig. 1b we are able to follow the evolution of the pulse area during one round-trip in the ring laser.

Let us now suppose that a short pulse with the small initial area $\Phi_0 \ll \pi$ enters the gain section (point 1 on the red (amplifier) curve 1g). As the pulse propagates in the amplifier, the corresponding point on the diagram is moving from right to left along the amplifier branch to the point 2, which is accompanied by an increase of the pulse area as one can see from Fig. 1b. After the pulse passes the amplifier, it is reflected by a non-ideal mirror and its area is thus reduced, which corresponds to the

moving the point on the diagram Fig. 1b vertically from 2 by some amount depending on r . Then, by moving along the straight line parallel to the horizontal axis one places the point to 3 on the absorber branch, which now describes the pulse entering the absorber. Evolution of the pulse in the absorber is described by moving from left to right along the blue branch until the point 4 where the pulse leaves the absorber. Now this point returns back to the gain branch at the point 5 thus closing the propagation circle. It continues to move further to the point 6 etc. Using such an approach one can expect that after many round-trips a stable limit cycle appears. This cycle and its formation is presented in Fig. 1c.

To confirm the results of our qualitative analysis presented above we perform numerical simulations based on a set of Maxwell-Bloch equations describing propagation of light in a two-level medium in a slow-varying envelope approximation [8, 9, 12–14]:

$$\partial_t p_s(z, t) = -\gamma_2(z) p_s(z, t) + g(z) n(z, t) A(z, t), \quad (2)$$

$$\partial_t n(z, t) = -\gamma_1 [n(z, t) - N_0(z)] - F(z, t), \quad (3)$$

$$\partial_t A(z, t) + c \partial_z A(z, t) = \kappa(z) p_s(z, t), \quad (4)$$

where $g(z) = \frac{d(z)}{2\hbar}$, $\kappa(z) = -4\pi\omega_0(z)d(z)N_0(z)$, $F(z, t) = 4g(z)A(z, t)p_s(z, t)$, $p_s(z, t)$ is the slowly varying envelope of imaginary part of non-diagonal element of the quantum mechanical density matrix of a two level particle, $n(z, t)$ is the population difference between the lower and upper energy levels, $A(z, t)$ is the slowly varying amplitude of the electric field. The equations include parameters of the two-level particles, such as transition dipole moment $d(z)$, concentration of two-level particles $N_0(z)$, population difference relaxation time $T_1(z) = 1/\gamma_1(z)$, polarization relaxation time $T_2(z) = 1/\gamma_2(z)$ and transition frequency of the two-level medium $\omega_0(z)$. We also assume that $g(z)$ is a constant in every piece of the cavity defined, namely $g(z) \equiv g_a$ in the absorption medium and $g(z) \equiv g_g$ in the gain medium (and analogously for $\kappa(z)$, $d(z)$, $N_0(z)$, $\omega_0(z)$, each of them obtains an index a or g in the corresponding medium). In particular, $N_{0g} = -1$, $N_{0a} = 1$. The set of equations (2)-(4) allows accurate

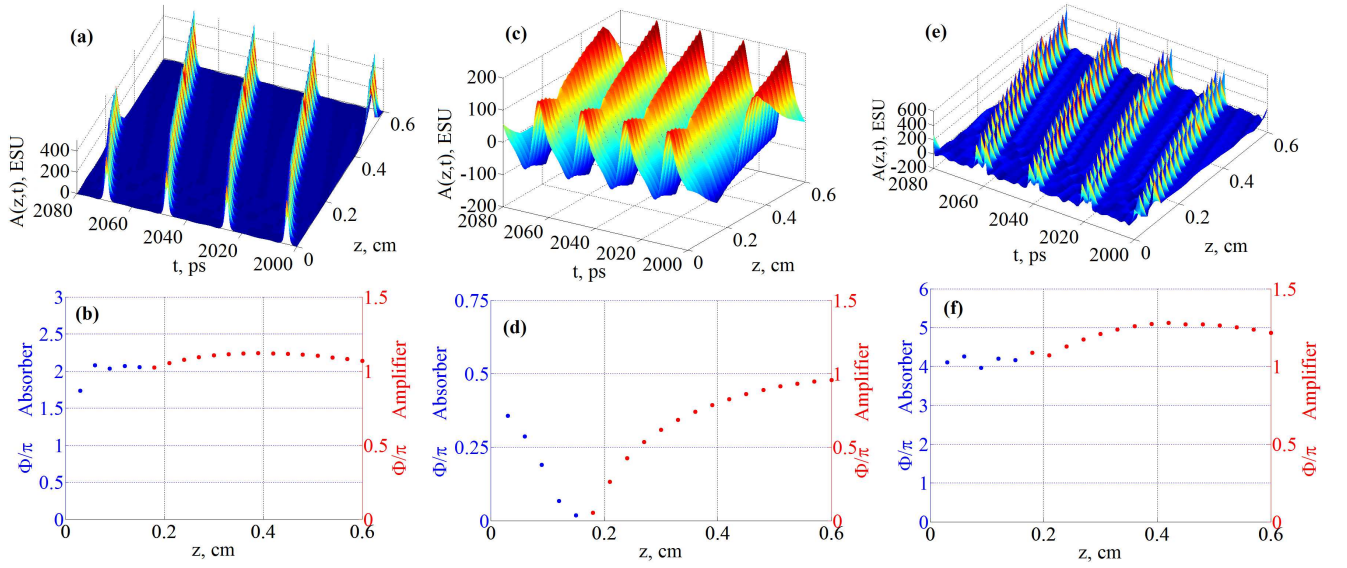


FIG. 2. (a),(c),(e): Distribution of the electric field amplitude $A(z)$ in the cavity for different values of m_d : (a): $m_d = 2$, (c): $m_d = 0.5$, (e): $m_d = 4$. (b),(d),(f): Evolution of the pulse area in the cavity during one round-trip for different values of m_d : (b): $m_d = 2$, (d): $m_d = 0.5$, (f): $m_d = 4$. The other parameters are the following: Central wave length $\lambda_{a,g} = 0.7 \mu\text{m}$, reflectivity of the mirror $r = 0.8$, length of the medium $L_g = 0.45 \text{ cm}$, $L_a = 0.15 \text{ cm}$, $d_g = 5 \text{ Debye}$, $N_{0g} = N_{0a} = 12.5 \cdot 10^{14} \text{ cm}^{-3}$, $T_{1g} = T_{1a} = 0.16 \text{ ns}$, $T_{2g} = T_{2a} = 40 \text{ ps}$. High values of T_2 (units and hundreds of ps) can be obtained in quantum dots at low temperatures [17].

modeling of evolution of extended two-level media in a cavity assuming relatively long (up to 100 fs) pulse durations and low intensities (Rabi frequency $\Omega_R \ll \omega_0$), so that no significant intracavity dispersion effects and no multilevel dynamics enter into play. The equations take also into account longitudinal multi-mode dynamics and the nonlinear coherent effects accompanying interaction of the light with the two-level particles. We use the system of equations (2)-(4) to analyze the dynamics of the ring CML laser assuming the regime of unidirectional propagation far away from the single-cycle limit.

Fig. 2a shows the distribution of the electric field amplitude $A(z)$ in the cavity over 100 round-trips in a steady-state when absorber/gain dipole moment ratio $m_d \equiv d_a/d_g = 2$. Fig. 3b illustrates the dependence of the pulse area inside the cavity during a single pass. It is clearly seen that, as it was predicted above, the pulse area is close to 2π in the absorber and to π in the gain. It is remarkably that in the present case the pulse area decreased due to the reflection from the mirror is restored in the absorber. Besides the pulse area in the amplifier changes nonmonotonically. In general however, the stable regime do establishes with the pulse area dynamics as predicted in Fig. 1c. It can be also seen in Fig. 2a that the pulse velocity in the absorber is smaller than in the amplifier, which manifests itself in a bend of the pulse propagation trajectory on the boundary between the absorber and amplifier.

With the help of the diagrams introduced above we will extend our consideration to a more general situation when the ratio of the dipole moments is not equal to

two. First, we consider the case when $m_d < 1$. The corresponding diagram for $m_d = 0.5$ is shown in Fig. 3a. In this case the limit cycle is realized with the branch 1g of the amplifier and 1a of the absorber. On the amplifier branch, the pulse with the area tending to π is formed, whereas the absorber decreases the pulse area almost to zero (see Fig. 2d). Because of the energy conservation, pulse envelope must change its sign (see Fig. 2c), and hence, 0π pulse is formed [18]. In the example presented in Fig. 3b, in contrast, we set $m_d = 1.5$. In this case, the branch 1g of amplifier and one of the branches 1a or 2a of the absorber can take part in the generation. In both of these possibilities the dynamics in the amplifier section is similar whereas in the absorber the pulse duration can increase (branch 2a). The situation when m_d is further increased and achieves $2 < m_d < 3$, namely, $m_d = 2.5$ is shown in Fig. 3c. One branch of the amplifier 1g and one of the three branches of the absorber 1a, 2a or 3a will be involved in this case. The cycle formed on the branch 3a yields a reduction of the pulse duration, because the pulse just before the absorber has the area $\Phi > 2\pi$. Thus, the ratio of the dipole moments influences the pulse duration and its dynamics in the CML cycle. The decrease of the pulse duration with the increase of m_d was predicted theoretically in [8, 9].

In the situation when $m_d > 3$ the branch 4a and 1g can participate in generation (Fig. 3d). On this branch, the formation of 4π -pulses takes place, which are, however, as our simulations show (see Fig. 2e,f), split into two 2π pulses having typically different amplitudes and durations. That is, two pulses over a single cavity round-trip

arise. The physical reason of this splitting can be easily understood from the fact that each 2π "part" causes excitation and de-excitation of the medium. Therefore, the central part of the pulse is continuously interacting with the particles which have returned to the ground state and hence is gradually "eaten" [20].

Note, that in numerical simulations we used parameters typical for quantum dots (QDs) (relaxations times, dipole moments etc). We remark that semiconductor QDs seems to be appropriate candidates for experimental observation of CML regime because of large values of dipole moments as well as large low-temperature relaxation times T_2 (in excess of 500 ps) [17].

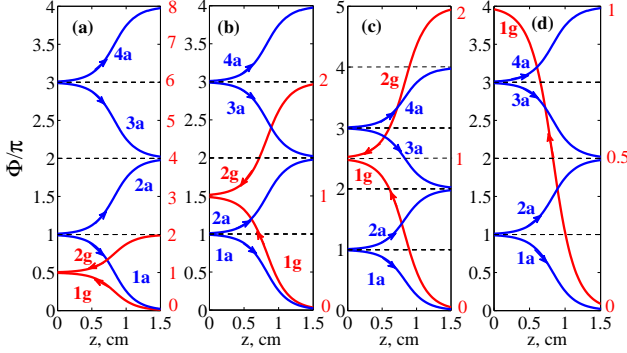


FIG. 3. Branches of solution of Eq. (1) for the absorber (blue lines) and amplifier (red lines) for different values of m_d . (a): $m_d = 0.5$, (b): $m_d = 1.5$, (c): $m_d = 2.5$, (d): $m_d = 4.0$

The diagrams presented above allow to calculate some characteristics of the pulse analytically. The evolution of the pulse area at some point (for instance, just at the entrance the gain section) $\Phi_{n+1}^{(a)} = \frac{d}{h} \int \mathcal{E} dt$ at the step $n + 1$ can easily related to $\Phi_n^{(a)}$ as $\Phi_{n+1}^{(a)} = F(\Phi_n^{(a)})$,

$$F(\Phi) = 2 \arctan \left[e_a \tan \left\{ r m_d \arctan \left(e_g \tan \left\{ \frac{\Phi}{2m_d} \right\} \right) \right\} \right], \quad (5)$$

where $e_a = \exp(-\alpha_a L_a/2)$, $e_g = \exp(\alpha_g L_g/2)$ [21]. This expression allows to consider the mode-locking regime as a fixed point of the mapping F which is stable if $|F'| \equiv |dF/d\Phi| < 1$.

Although in general F (and thus F') can be calculated only numerically, analytical results can be obtained assuming small deviation of e_a , e_g and r from one (as it is usually happens in a typical laser). In this case, we denote $e_a = 1 - \epsilon_a$, $e_g = 1 + \epsilon_g$, $r = 1 - \epsilon_r$ and assume $|\epsilon_{g,a,r}| \ll 1$, $\epsilon_{g,a,r} > 0$. We also must select the branches of $\tan(x)$ and $\arctan(x)$ which make F continuous in the vicinity of the fixed point. For instance, near non-lasing point $\Phi = 0$ we obtain (by taking derivative of Eq. (5) and expanding into series in $\epsilon_{g,a,r}$):

$$|F'| = 1 - \epsilon_a + \epsilon_g - \epsilon_r + \dots, \quad (6)$$

where (...) means the higher order terms in $\epsilon_{g,a,r}$. That

is, in the linear approximation, the expression for $1 - |F'|$ reproduces the loss-gain balance in the system.

Furthermore, for a CML regime with $m_d = 2$ we may assume the fixed point is close to 2π , that is, $\Phi^{(a)} = 2\pi + \epsilon$, $\epsilon \ll 1$ which, by substitution into Eq. (5), allows us to obtain in the lowest order: $\epsilon = -2\pi\epsilon_r/(\epsilon_a + \epsilon_g + \epsilon_r) + \dots$. This expression can be singular, indicating that for $\epsilon_r = \text{const}$ and $\epsilon_{g,a,r} \rightarrow 0$ the fixed point near $\Phi^{(a)} \approx 2\pi$ disappears. To ensure $\epsilon \ll 1$ a regularizing expansion is needed. For instance, we may introduce the parameter δ such that $\epsilon_a = a\delta$, $\epsilon_g = g\delta$, $\epsilon_r = \rho\delta^2$; $0 < a, g, \rho \ll 1/\delta$. With this expansion we obtain:

$$\epsilon = \frac{-2\pi\rho}{a+g}\delta + O(\delta^2), \quad (7)$$

which, in turn, gives us:

$$|F'| = 1 - (a+g)\delta + O(\delta^2), \quad (8)$$

that is, because $a, g > 0$, the CML regime is always stable in the lowest order (assuming it exists and $\epsilon \ll 1$). In particular, this point is becoming the only attracting one if the nonlasing state is unstable, thus giving rise to CML directly at threshold. Although the stability of the corresponding cycle does not automatically ensures the stability of the fundamental mode-locking regime because instability at nonzero wavenumber can arise, we can often take the cavity short enough to suppress such instabilities as was shown in [9].

In conclusion, we developed a diagram technique, allowing to study the CML regimes qualitatively, and demonstrated existence of stable limit cycles in the system, corresponding to CML regimes. Moreover, our results show that such regimes can appear directly at the laser threshold. Although the area theorem is applicable for the case of large T_2 , practically "large" means only that $T_2 \gg$ the round-trip time. Our numerical simulations show also that the predictions of the theory are valid even if these times are comparable (but still T_2 is not too small). We also extended the CML to the case when m_d , the ratio of the transition dipole moments of the absorber and the gain media is arbitrary. In contrast to previously considered 2π configurations, in this case, 0π pulses as well as $2n\pi$ pulses can be obtained. The later can be called super-CML because more than one Rabi oscillation per cavity round-trip appears. Such $2n\pi$ pulses are however unstable and split into n sub-pulses, each of them having area 2π . Although CML has not been realized experimentally yet, the most of the basic aspects of SIT including the area theorem were verified experimentally [11, 13, 18, 19]; In particular, coherent phenomena were recently observed in quantum dots [22, 23]. Thus, we hope that the present letter will facilitate further efforts on its experimental realization.

FUNDING INFORMATION

This work was partially financially supported by Government of Russian Federation, Grant 074-U01.

-
- [1] U. Keller, “Ultrafast solid-state laser oscillators: a success story for the last 20 years with no end in sight,” *Appl. Phys. B* **100**, 15 (2010).
 - [2] V. V. Kozlov, “Self-induced transparency soliton laser via coherent mode locking,” *Phys. Rev. A* **56**, 1607 (1997).
 - [3] V. V. Kozlov, “Self-induced-transparency soliton laser,” *JETP Lett.* **69**, 906 (1999).
 - [4] C. R. Menyuk and M. A. Talukder, “Self-induced transparency mode-locking of quantum cascade lasers,” *Phys. Rev. Lett.* **102**, 023903 (2009).
 - [5] M. A. Talukder and C. R. Menyuk, “Analytical and computational study of self-induced transparency mode locking in quantum cascade lasers,” *Phys. Rev. A* **79**, 063841 (2009).
 - [6] V. V. Kozlov, N. N. Rosanov, and S. Wabnitz, “Obtaining single-cycle pulses from a mode-locked laser,” *Physical Review A* **84**, 053810 (2011).
 - [7] V. V. Kozlov and N. N. Rosanov, “Single-cycle-pulse passively-mode-locked laser with inhomogeneously broadened active medium,” *Phys. Rev. A* **87**, 043836 (2013).
 - [8] R. M. Arhipov, M. V. Arhipov, and I. V. Babushkin, “On coherent mode-locking in a two-section laser,” *JETP Lett.* **101**, 149–153 (2015).
 - [9] R. M. Arhipov, M. V. Arhipov, and I. Babushkin, “Self-starting stable coherent mode-locking in a two-section laser,” *Optics Communications* **361**, 73–78 (2016).
 - [10] S. L. McCall and E. L. Hahn, “Self-induced transparency by pulsed coherent light,” *Phys. Rev. Letters* **18**, 908 (1967).
 - [11] S. L. McCall and E. L. Hahn, “Self-induced transparency,” *Physical Review* **183**, 457 (1969).
 - [12] P. G. Kryukov and V. S. Letokhov, “Propagation of a light pulse in a resonantly amplifying (absorbing) medium,” *Physics-Uspekhi* **12**, 641 (1970).
 - [13] L. Allen and J. H. Eberly, *Optical resonance and two-level atoms* (Wiley, New York, 1975).
 - [14] G. Lamb Jr, “Analytical descriptions of ultrashort optical pulse propagation in a resonant medium,” *Rev. Mod. Phys.* **43**, 99 (1971).
 - [15] N. Vysotina, N. Rosanov, and V. Semenov, “Extremely short dissipative solitons in an active nonlinear medium with quantum dots,” *Opt. Spectr.* **106**, 713 (2009).
 - [16] M. V. Arhipov, R. M. Arhipov, A. A. Shimko, and I. Babushkin, “Mode-locking in a laser with a coherent absorber,” *JETP Lett.* **101**, 232 (2015).
 - [17] P. Borri, W. Langbein, S. Schneider, U. Woggon, R. L. Sellin, D. Ouyang, and D. Bimberg, “Ultralong dephasing time in ingaas quantum dots,” *Phys. Rev. Lett.* **87**, 157401 (2001).
 - [18] J. E. Rothenberg, D. Grischkowsky, and A. C. Balant, “Observation of the formation of the zero-area pulse,” *Phys. Rev. Lett.* **53**, 552 (1984).
 - [19] J. Schüttler, I. Babushkin, W. Lange, “Labyrinthine patterns on an inhomogeneous background in a nonlinear optical system,” *Phys. Rev. A*, **78**, 035802 (2008).
 - [20] I. Poluektov, Y. M. Popov, and V. Rouitberg, “Self-induced transparency effect,” *Soviet Physics Uspekhi* **17**, 673 (1975).
 - [21] I. V. Babushkin, Y. A. Logvin, and N. A. Loiko, “Interrelation of spatial and temporal instabilities in a system of two nonlinear thin films,” *J. Exp. Theor. Phys.* **90**, 133 (2000).
 - [22] O. Karni, A. Capua, G. Eisenstein, V. Sichkovskiy, V. Ivanov, and J. P. Reithmaier, “Rabi oscillations and self-induced transparency in InAs/InP quantum dot semiconductor optical amplifier operating at room temperature,” *Opt. Expr.* **21**, 26786 (2013).
 - [23] M. Kolarczik, N. Owschimikow, J. Korn, B. Lingnau, Y. Kaptan, D. Bimberg, E. Schöll, K. Lüdge, U. Woggon, “Quantum coherence induces pulse shape modification in a semiconductor optical amplifier at room temperature,” *Nat. Comm.* **4**, 1 (2013).